IMPROVING HYDROGRAPHIC PPP BY HEIGHT CONSTRAINING

Ashraf ABDALLAH and Volker SCHWIEGER

Keywords: Kinematic GNSS-PPP, Height constraining, Hydrographic survey, Bernese software

SUMMARY

The GNSS PPP (Precise Point Positioning) technique has received a considerable attention to obtain cost-effective and accurate positions. Recently, this technique is one of the most significant techniques to obtain hydrographic information. Since, theoretically, the shallow water resources have a stable water level, the idea of this paper is to improve the 2D positions assuming stable water level. Three hydrographic trajectories are processed in this study, which provided an $RMS_{2D\ position}$ of 7 cm – 10 cm for the original PPP solution without this assumption. Two different constraining procedures are applied: the first one aims to constrain the whole trajectory at one water level. One hydrographic trajectory, which was surveyed on the Rhine River, is investigated. Due to the variation of the height of more than 60 cm, the solution does not deliver any enhancement in the accuracy. The second procedure purposes to constrain the height for a piecewise stability. The piecewise sessions are automatically detected according to a specific number of epochs and a defined standard deviation. Three hydrographic trajectories are tested; two trajectories were observed on the Rhine River. After height constraining, these trajectories show an improved $RMS_{2D\ position}$ in between 20% and 35%. The third trajectory was observed on the Nile River. The constraining procedure provides an improvement of the $RMS_{2D\ position}$ of 16%. Generally, the achieved $RMS_{2D\ position}$ after applying the height constraining for the three trajectories is 4.7 cm to 8 cm.

IMPROVING HYDROGRAPHIC PPP BY HEIGHT CONSTRAINING

Ashraf ABDALLAH and Volker SCHWIEGER

1. INTRODUCTION

Since Zumberge et al. (1997) have developed at the Jet Propulsion Laboratory (JPL) the first efficient method for the PPP estimation of GPS data, there is great interest to increase the positioning accuracy with a cost-effective technique. In order to achieve highly accurate coordinates, various errors have to be modelled or eliminated. These errors can be classified into (1) satellite dependent errors that are related to the satellite clocks and orbits, satellite phase centre variation, and antenna phase wind-up, (2) receiver dependent errors, which consist of the antenna phase centre variation and the receiver clock errors, (3) atmospheric errors, which include the ionosphere and troposphere zenith delay. (4) For a more accurate estimation, ocean tide loading, earth rotation parameters, and atmospheric tidal loading are considered in the PPP estimation: Héroux and Kouba (2001), El-Rabbany (2002), Rizos (2010) and Mirsa and Enge (2012).

Since the GNSS technique provides the position of objects with high accuracy (Hoffmann-Wellenhof et al., 2000), this technique has become one of the most important techniques to obtain hydrographic information. Mainly, hydrographic applications have two measurements: positioning including attitude determination and the water depth measurement (Erener and Gökalp, 2004). There are two significant goals of measuring the water depth. The first goal aims to compute the mud and sedimentation levels of the concerned water resource. This mud level can affect the navigation way for ships and influences the under-keel clearance (UKC). The UKC is the distance between the bed of a ship and the bed of the water resource. The second goal is to detect obstacles under the water surface like cars or ships, so these obstacles can quickly be released to clear the water resource (Michaud et al., 2002). A bathymetric survey can introduce a reliable method to detect e.g. the archeological objects under water with a high accuracy (Böder, 2010). Therefore, a better estimation of the position of surveying vessels is leading to more precise horizontal coordinates for the corresponding water depth.

One of the properties of the shallow water resources is that the water level is approximately stable. This characteristic is the base for an approach to constrain the height component to improve the $2D_{position}$. This concept provides an advantage for hydrographic surveying. In addition, no previous literature has investigated this concept to improve the estimated PPP $2D_{position}$ for the hydrographic applications. Therefore, an open research area to improve the $2D_{position}$ of hydrographic objects is identified. This paper introduces a new approach for height constraining using Bernese GNSS software that has been developed by the Astronomical Institute of the University of Bern (AIUB), Switzerland.

2. MATHEMATICAL MODEL

The key aspect of the PPP estimation depends on the use of the ionosphere-free linear combination. Since the precise satellite orbit and clock data are provided by the International GNSS Service (IGS), the satellite clock error δ^S and the satellite position x_S, y_S, z_S are precisely known. The estimation equations can be written as seen in equation (1) and (2).

$$\rho_{IF} = r + c\delta^R - c\delta^S + T_z \cdot m(E) + \varepsilon_\rho = 2.546\rho_{L1} - 1.546\rho_{L2}, \quad (1)$$

$$\Phi_{IF} = r + c\delta^R - c\delta^S + T_z \cdot m(E) + \lambda_{IF} \cdot N_{IF} + \varepsilon_\Phi = 2.546\Phi_{L1} - 1.546\Phi_{L2}, \quad (2)$$

where:

Φ_{IF} & ρ_{IF} : ionosphere-free linear combination for carrier phase and code data,

ϕ_{L1} & ϕ_{L2} : carrier phase for the signals L_1 & L_2,

ρ_{L1} & ρ_{L2} : code data for the signals L_1 & L_2,

r : true geometric range between the satellite and receiver x_R, y_R, z_R,

c : speed of light in vacuum,

δ^R : receiver clock error,

$T_z \cdot m(E)$: troposphere refraction including mapping function,

λ_{IF} : combined carrier wavelength,

N_{IF} : combined float ambiguity integers,

ε_ρ , ε_ϕ : relevant measurement noises, including the multipath.

The traditional PPP estimation is carried through by a least square adjustment. This estimation methodology is the one which is used in the Bernese GNSS software. The linearized form of the estimation is shown in equation (3). This equation is the basic formula of the Gauss-Markov Model (Niemeier, 2008).

$$\boldsymbol{l} + \boldsymbol{v} = \boldsymbol{A} \cdot \hat{\boldsymbol{x}}, \tag{3}$$

where:

$\boldsymbol{l}$: reduced observation vector ($n \times 1$),

$\boldsymbol{v}$: residual vector ($n \times 1$),

$\boldsymbol{A}$: design matrix ($n \times u$),

$\hat{\boldsymbol{x}}$: vector of unknown parameters ($u \times 1$),

$n \times u$: number of observations, number of unknown parameters.

The estimated vector of unknowns $\hat{\boldsymbol{x}}$ is estimated in equation (4) (Dach et al., 2007 and Niemeier, 2008).

$$\hat{\boldsymbol{x}} = (\boldsymbol{A}^T \boldsymbol{P}_l \boldsymbol{A})^{-1} \cdot \boldsymbol{A}^T \boldsymbol{P}_l \boldsymbol{l} = \boldsymbol{N}^{-1} \cdot \boldsymbol{n}, \tag{4}$$

where:

$\boldsymbol{N}$: normal equation matrix,

$\boldsymbol{n}$: right hand of the normal equation matrix,

$\boldsymbol{P}_l$: weight matrix.

In the case of the height constraining concept, the constraining parameters are added to the normal equation matrix $\boldsymbol{N}$ in the Gauss-Markoff Model, consequently, the exterior information regarding the constraining parameters is introduced as can be seen in equation (5) (Dach et al., 2007).

$$\boldsymbol{h} + \boldsymbol{v}_h = \boldsymbol{H} \cdot \hat{\boldsymbol{x}}, \tag{5}$$

where:

$\boldsymbol{h}$: vector of pseudo-observations / constrained parameters (r × 1),

$\boldsymbol{v}_h$: vector of residuals vector (r × 1),

$\boldsymbol{H}$: matrix with given coefficients (r × u) with rank H = r,

$\hat{\boldsymbol{x}}$: vector of unknown parameters (u × 1),

$r \times u$: number of constraints, number of unknown parameters.

The model of constrained parameters may be considered as an additional pseudo-observation to the main estimation model. Therefore, the estimation model in equation (3) can be updated to perform the following observation equation (6) with a co-factor matrix that is shown in equation (7):

$$\begin{bmatrix} \boldsymbol{l} \\ \boldsymbol{h} \end{bmatrix} + \begin{bmatrix} \boldsymbol{v}_l \\ \boldsymbol{v}_h \end{bmatrix} = \begin{bmatrix} \boldsymbol{A} \\ \boldsymbol{H} \end{bmatrix} \cdot \hat{\boldsymbol{x}}, \tag{6}$$

$$\mathrm{D}\left(\begin{bmatrix} \mathrm{l} \\ \mathrm{h} \end{bmatrix}\right) = \sigma^2 \begin{bmatrix} \mathrm{P_l}^{-1} & 0 \\ 0 & \mathrm{P_h}^{-1} \end{bmatrix}. \tag{7}$$

The related normal equation system is described in equation (8)

$$(\boldsymbol{A}^T \boldsymbol{P}_l \boldsymbol{A} + \boldsymbol{H}^T \boldsymbol{P}_h \boldsymbol{H}) \cdot \hat{\boldsymbol{x}} = \boldsymbol{A}^T \boldsymbol{P}_l \boldsymbol{l} + \boldsymbol{H}^T \boldsymbol{P}_h \boldsymbol{h}. \tag{8}$$

$\boldsymbol{P}_h$ is the weight matrix of constraints that is defined in equation (9). σ_0 refers to the a priori sigma; this value is set to 1 mm in Bernese GNSS software. σ_i refers to the input sigma for the parameters to be constrained. Concerning this study, only the height is constrained with different standard deviations or adapted ones. During the estimation, the input sigma for the horizontal direction ($\sigma_\varphi^2, \sigma_\lambda^2$) is set to 100, which means that the horizontal components are not constrained. Otherwise, for the height component (σ_h^2), the inserted sigma is defined according to the constraining procedure.

$$\boldsymbol{P}_h = \sigma_0^2 \begin{bmatrix} \frac{1}{\sigma_\varphi^2} & 0 & 0 \\ 0 & \frac{1}{\sigma_\lambda^2} & 0 \\ 0 & 0 & \frac{1}{\sigma_h^2} \end{bmatrix} \tag{9}$$

The matrix $\boldsymbol{H}$ refers to the Jacobian matrix for the relationship between the ellipsoidal and Cartesian coordinates (Dach et al., 2007). If the constraining would be realized in the ellipsoidal system, the matrix $\boldsymbol{H}$ would be the unit matrix.

$$\boldsymbol{H} = \begin{bmatrix} \frac{\partial \varphi}{\partial x} & \frac{\partial \varphi}{\partial y} & \frac{\partial \varphi}{\partial z} \\ \frac{\partial \lambda}{\partial x} & \frac{\partial \lambda}{\partial y} & \frac{\partial \lambda}{\partial z} \\ \frac{\partial h}{\partial x} & \frac{\partial h}{\partial y} & \frac{\partial h}{\partial z} \end{bmatrix} \tag{10}$$

3. GNSS SOLUTION AND COORDINATE CONSTRAINING USING BERNESE SOFTWARE

Bernese GNSS Software, Version 5.2 is a high-quality geodetic software package. It is widely used for geodetic networks estimation in postprocessing for various aspects. In addition, it has the potential to process GNSS data for static and kinematic applications. Moreover, it processes the measurement data in double-difference (Differential GNSS estimation), and zero-difference (PPP solution estimation) (Dach et al., 2007). Complete documentation of the software can be obtained from the official website under (http://www.bernese.unibe.ch/). Dach et al. (2007) provide the user manual; Dach and Walser (2015) show a course tutorial including processing examples, introductory course, and a terminal session. This tutorial is always updated. The processing schedule for PPP and double-difference solution as well as the processing parameters are explained in Abdallah & Schwieger (2015).

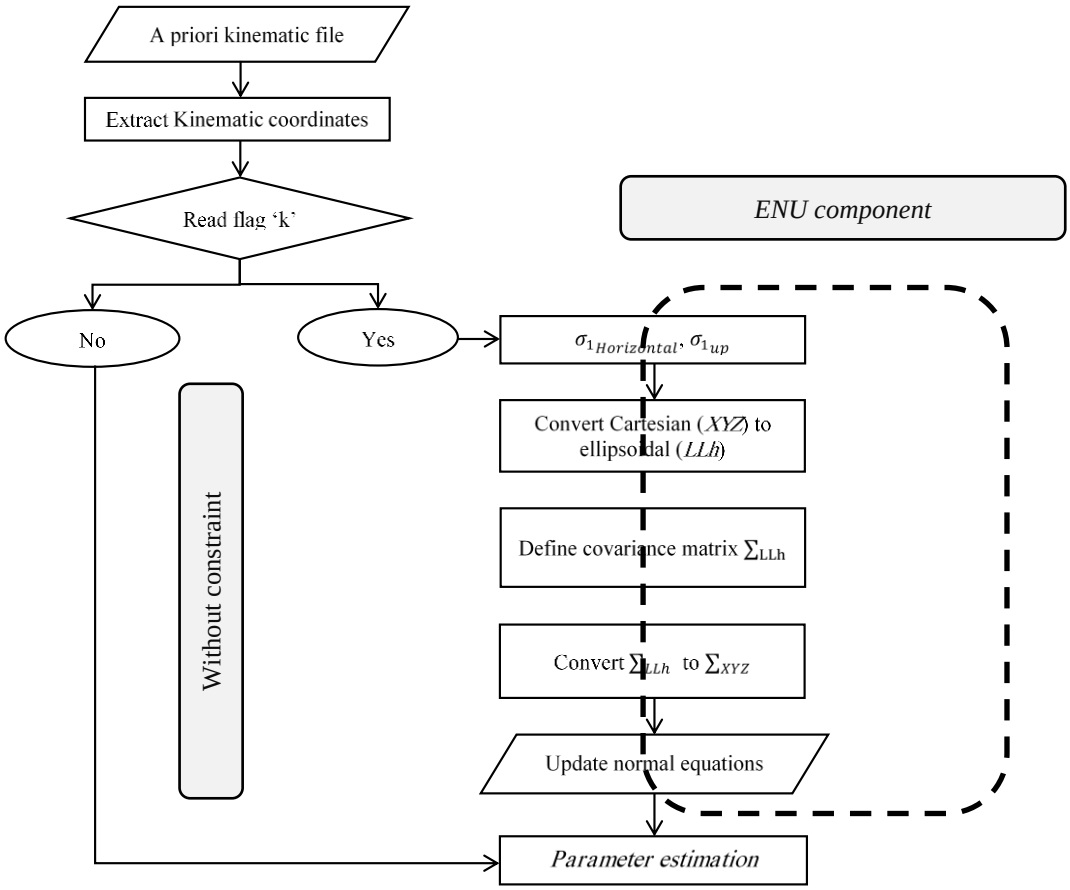

Figure 1: Constraining using Bernese software (Abdallah, 2016)

Bernese GNSS software provides the possibility to constrain the kinematic coordinates with respect to a priori trajectory. A general flowchart of the constraining using Bernese GNSS software is presented in Figure 1. The procedure of constraining mainly depends on a priori kinematic trajectory. This kinematic trajectory contains the Cartesian coordinates (XYZ). The Cartesian coordinates are extracted from the a priori kinematic file with a flag. There are three flags within Bernese software. Flag 'K' means that the coordinates are well estimated in the kinematic mode. Flag 'X' means that the coordinates are not estimated and flag 'S' means that the coordinates are interpolated. The constraining for the kinematic mode is only running with the 'K' flag. Thus, if the software reads the flag of 'X' or 'S, the solution will be estimated without any constraints (DACH, et al., 2007).

The coordinates are constrained in ENU (Longitude, Latitude, height) plan; in this case, one sigma for horizontal ($\sigma_{\varphi}^2, \sigma_{\lambda}^2$) and one for the vertical components (σ_h^2) has to be inserted into the software. The a priori Cartesian kinematic coordinates are transformed to ellipsoidal coordinates (latitude, longitude, height). Then the covariance matrix for the ellipsoidal coordinates is defined with a priori sigma for constraining σ_1^2 and the a priori sigma of observation data σ_0^2. The defined covariance matrix for ellipsoidal coordinates $\sum_{LLh}$ is

transformed to the covariance matrix for Cartesian coordinates $\sum_{XYZ}$. Finally, the normal equations $\boldsymbol{N}$ are updated by including the constraint values and then the parameters are estimated (Abdallah, 2016).

4. EXPERIMENTAL WORK

Three hydrographic trajectories are considered in this paper. Two trajectories have been observed on the Rhine River, Duisburg Harbor, Germany. An antenna of LEICA X1203+GNSS and a receiver LEICA GX1230+GNSS are located on the surveying vessel to collect the GNSS data. Figure 2 shows the location of the GNSS antenna on the surveying vessel. The virtual SAPOS (SAtellitenPOSitionierungsdienst der Deutschen Landesvermessung) reference station was considered as a reference station; it was provided from SAPOS-NRW team (SAPOS-NRW, 2016). SAPOS service is collecting GNSS data around Germany (SAPOS, 2016). Here it is used for the differential GNSS solution only. The third trajectory was measured on the Nile River, Aswan, Egypt. A GNSS antenna of Leica15 Viva is connected to a GPS pole on a small ship; the antenna on the ship is shown in Figure 3. To obtain a reference solution, a CORS station is used that is located in the Earthquake Centre in Sahary region beside the high dam, Aswan, Egypt. Table 1 presents the characteristics of the experimental data. Figure 4 and Figure 5 show the location of the trajectories that are observed on the Rhine and Nile Rivers, respectively.

Table 1: Experimental work characteristics

ID	Country/ City	Year/ DOY	Start time			End time			Interval	Trajectory Length [km]
			hh	mm	ss	hh	mm	ss	ss	
1	Germany/ Duisburg	2014/126	07	40	00	10	10	05	05	10.70
2		2014/126	10	17	05	14	15	00	05	19.40
3	Egypt/ Aswan	2015/019	14	15	25	15	22	06	01	6.10

Figure 2: Observation vessel for the Rhine River data,

Mercator observation vessel (left photo); GPS antenna on the vessel (right photo),

Photos by: Annette Scheider (IIGS)


Figure 3: Observation vessel for the Nile River data,

Measurement ship (left photo), antenna of Leica 15 Viva (right photo)

Figure 4: Location of the first trajectory, Germany (2014/126),

© Google earth (Image: 30.06.2015)

Figure 5: Location of the third trajectory, Egypt (2015/019),

© Google earth (Image: 30.06.2015)

5. ANALYSIS AND RESULTS

Two processing procedures have been applied using Bernese software to identify the reliability of the height constraining for the hydrographic kinematic applications. The first procedure is based on the assumption of stability of the water level. The second procedure is based on the concept of piecewise stability of the water level.

5.1 Assumption of stability of the water level

The procedure assumes that the water level is stable during the measurements. Since the kinematic measurements for this study began with quasi-static observation data, the average coordinates of the first 10 minutes are considered as fixed coordinates for the whole trajectory.

Then, the a priori kinematic trajectory was created to be inserted for the constrained estimation. As a validation of this procedure, the first trajectory is processed with this concept. During the estimation, two sigma values have been applied: one with 1 mm, which means that no change in the height is allowed; the second with 5 cm, which means the maximum variation is 5 cm.

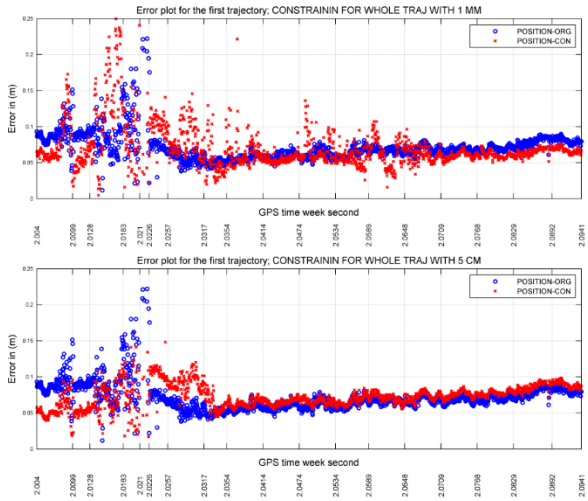

Figure 6: Results of stability of water level solution,

2D error plot with constraining sigma of 1 mm (upper plot); 2D error plot with constraining sigma of 5 cm (lower plot)

Figure 6 shows the $2D_{position}$ for the original PPP and constrained PPP solutions. The two solutions show an improved solution in the beginning. Afterwards, there is no significant improvement in the position by height constraining. The possible explanation for this performance is that the used mean height and sigma are not reflecting the reality of the whole trajectory. As to be shown in Figure 7, the height varies in the range of more than 60 cm.

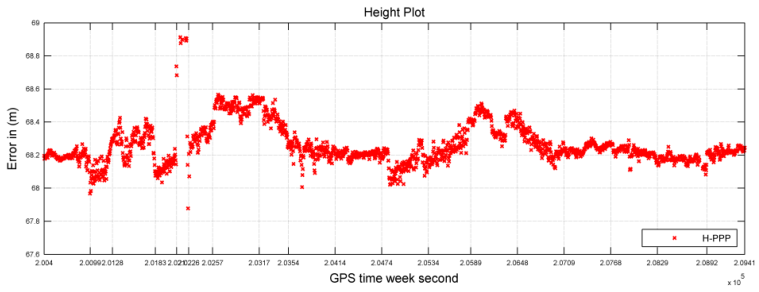

Figure 7: PPP height profile for the first trajectory

5.2 Assumption of piecewise stability of the water level

The previous assumption focussed on using one a priori height for the complete trajectory. The following one introduces a new implementation by considering different heights over time. The implementation is carried out using an automatic detection for the processed sessions utilizing a specified standard deviation for height variations and a defined number of epochs for each session. The following sections describe the procedure and the validity of the idea for the hydrographic measurements. The automatic detection for the piecewise stability of the water level aims to detect the short stability of the height. As shown in Figure 8, two steps are needed for this solution. The first step, realized by a MATLAB code, was to create sessions representing the piecewise stability, to define the constraining sigma and the length of each session piecewise, and in addition to create the a priori kinematic file. Step 2 is carried out using Bernese GNSS software to obtain the constrained PPP solution (Abdallah, 2016).

The next points describe the procedure of the new implementation:

- The kinematic PPP coordinate file that is estimated without constraining is inserted into the MATLAB program. The coordinates are transformed from Cartesian to ellipsoidal coordinates.
- The cumulative standard deviation (σ_i) is checked in comparison to the defined maximum value (σ_{max}). If this value is equal or less than the maximum value, then the length of the piecewise session (t_i) is checked. If not; the session is defined by (σ_{max}, t_i).
- Check the length of the session (t_i); if this time is equal or less than the maximum, go to the next session. If not; the session is defined by the standard deviation of (σ_i) and the maximum time (t_{max}).
- The average latitude, longitude, and height coordinates for a session are calculated; then these are transformed to Cartesian coordinates.
- An a priori kinematic file is created with flag 'K' for the respective session and flag 'X' for the other epochs. In this case, the constraining procedure will be done in Bernese software for the epochs that have the 'K' flag, and the other epochs are free of constraining.
- For the constrained PPP estimation, the created a priori file is inserted into Bernese software for the kinematic PPP estimation for height constraining with the estimated σ_i for height.
- The estimated 2D position after constraining is compared epoch by epoch with the double-difference solution for the same epochs.

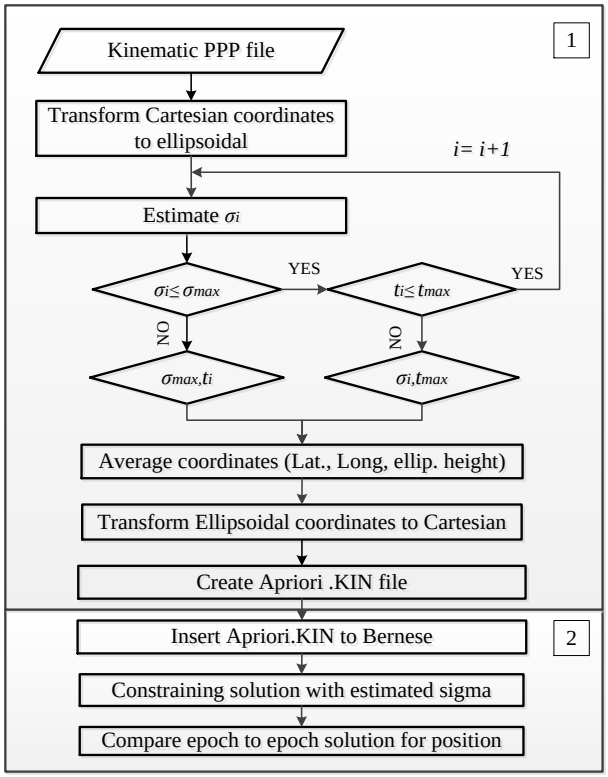

Figure 8: Flowchart for piecewise stability of water level constraining

The validation of this constraining procedure was applied for three trajectories. For the first two trajectories, the maximum selected time t_{max} was set to 10 minutes [120 epochs], and the σ_h was set to 7 cm; this value was found to be the best value to obtain an improved constrained solution. Due to the variation of the height profile in between 60 cm to 80 cm, the two trajectories were divided into 18 and 28 sessions, respectively.

Figure 9.a as well as Figure 10.a show the original PPP heights in blue dots for the first and second trajectory respectively. The red line refers to the considered mean heights for the processed sessions. It is apparent from this figure that there are some sessions having a number of processed epochs equal to the t_{max} of 120 epochs (marked with 1). In addition, some sessions have a number of epochs less than the maximum length due to the condition of the sigma value (marked with 2). Figure 9.b presents the $2D_{position}$ for the original PPP and constrained solutions for the first trajectory. In this figure, the blue circles indicate the estimated $2D_{position}$ for the original processing [without constraining]. On the other hand, the red cross points refer to the estimated $2D_{position}$ with constrained processing. It is obvious that there is a significant improvement in the estimated $2D_{position}$ after piecewise height constraining. Figure 10.b shows the whole $2D_{position}$ of the original PPP and constraint solution for the second trajectory. As shown in this figure, there is improvement in the position after constraining of height for most

epochs. Only the last epochs did not show an improved solution. In addition, there is a jump in the estimation due to a loss of data; this jump is marked with the dashed lines.

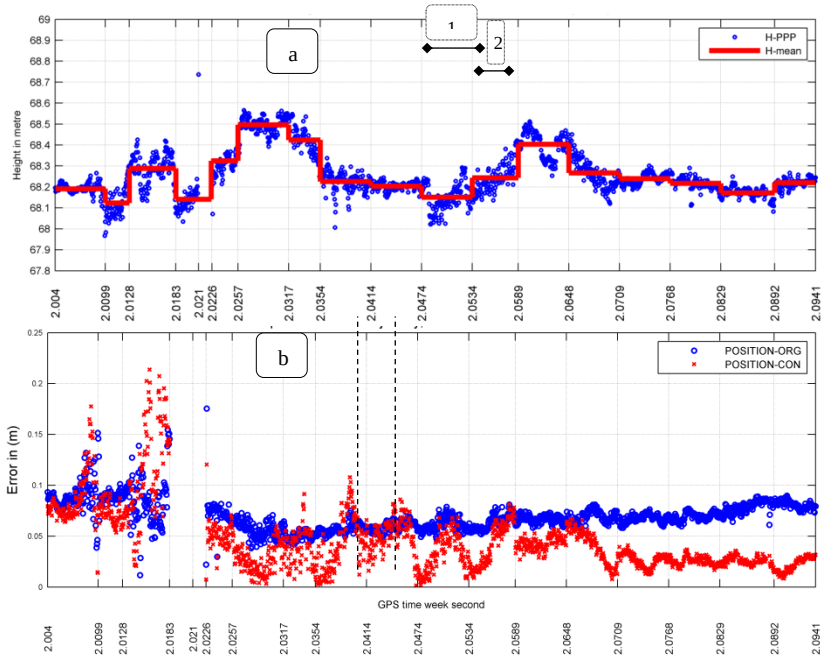

Figure 9: Heights, sessions and estimated positions for original and constraint solutions [first trajectory],

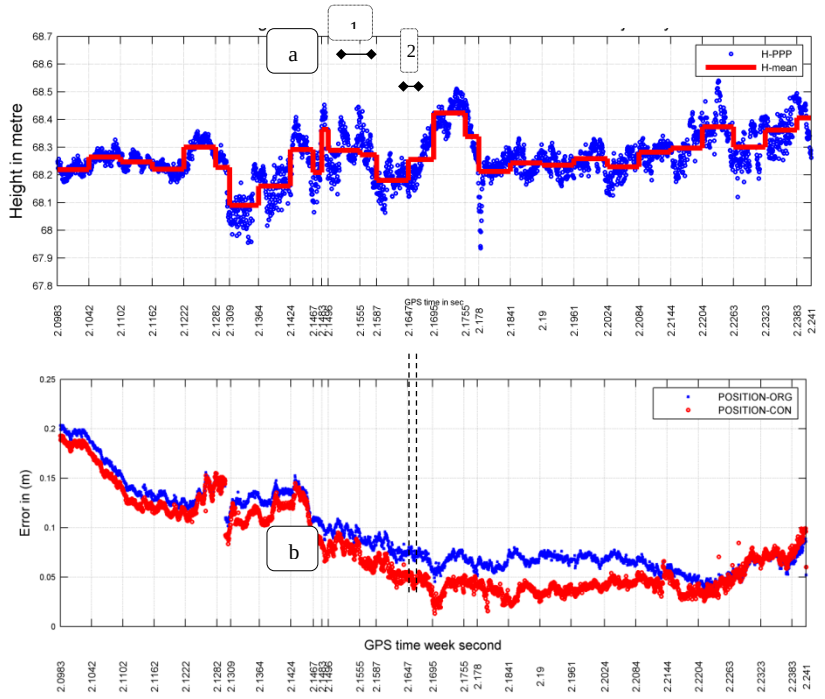

Figure 10: Heights, sessions and estimated positions for original and constraint solutions [second trajectory],

By applying the constraining procedure for the third trajectory, to obtain the best constrained solution, the used sigma σ_h for this data is 4 cm within a session length of 10 minutes, which equals to 300 epochs in this case. 14 sessions were detected for this constraining procedure. The relation between the PPP heights and the used mean heights is presented in Figure 11.a. Figure 11.b shows the estimated $2D_{position}$ without constraining and after constraining for the different sessions. It is obvious from this figure that there is an improvement for the constrained $2D_{position}$.

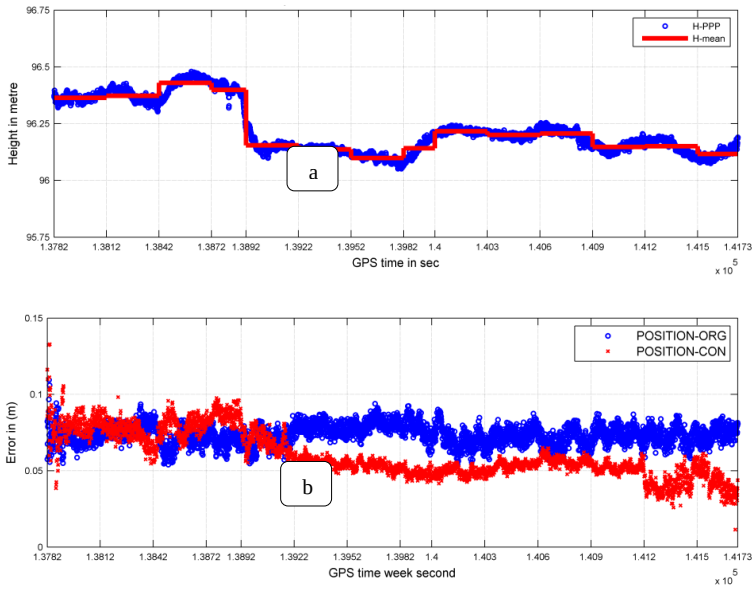

Figure 11: Heights, sessions and estimated positions for original and constraint solutions [third trajectory]

6. DISCUSSION AND CONCLUSION

As previously explained, the concept of complete stability of the water level did not provide any improvement in the $2D_{position}$. The possible explanation of this performance is due to the height variation of the measurement's vessel, which means that the considered mean height did not reflect the reality of the height profile. The assumption of piecewise stability of the water level provided a significantly improved $2D_{position}$ by height constraining. Figure 12 shows the estimated $RMS_{2D\ position}$ from the original and constrained solutions for the three trajectories. The first trajectory reported an $RMS_{2D\ position}$ of 7.2 cm for the original PPP solution; otherwise, the obtained one by constraining is 4.7 cm. That means an improvement of approximately 35 %. Regarding the second trajectory, the original solution shows an $RMS_{2D\ position}$ of 10 cm. On the other side, the constraint solution delivers an $RMS_{2D\ position}$ of 8.0 cm, which means 20 % improvement. With respect to the third trajectory, a 16 % improvement for the $2D_{position}$ after constraining is realized. The estimated $RMS_{2D\ position}$ for the original solution is 7.40 cm, whereas the delivered $RMS_{2D\ position}$ after constraining is 6.20 cm.

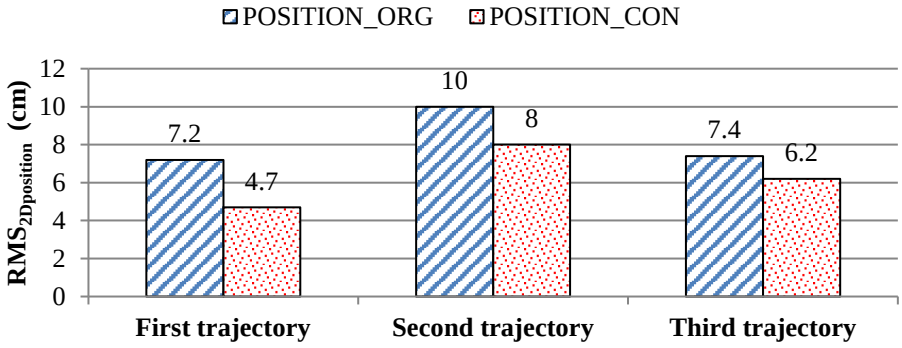

Figure 12: $RMS_{2D\ position}$ for original and constraint solutions

The main goal of the current study was to improve the 2D positions for the hydrographic PPP solutions by constraining the height. The paper has found that due to the variation of the water level during measuring, the concept of considering one water level did not provide generally an improvement in the 2D positions. The solution has been extended to implement a new procedure for height constraining by taking different stability sessions for the water level. This procedure has provided an improved $RMS_{2D\ position}$ of 16% to 35% after constraining the height.

ACKNOWLEDGEMENTS

The authors would like to thank Ms. Annette Scheider for receiving the GNSS measurements through the HydrOs project. Special thanks go to our partners from the BfG, Mr. Harry Wirth and Mr. Marc Breitenfeld. Further thanks also to Mr. Bernhard Galitzki from SAPOS-NRW for providing us with the reference station. Further thanks to the Faculty of Engineering, Aswan for providing us with the GPS instruments to collect the data on the River Nile. Deep thanks also go to Prof. Dr. Eng. Mostafa Rabah, the head of Crustal Movement Lab., National Research Institute of Astronomy & Geophysics, Egypt, for providing us with the reference station data in Aswan city, Egypt. The authors would like to thank the Egyptian Higher Education Ministry and the German Academic Exchange Service (DAAD) in Germany for the funding of the Ph.D. research.

REFERENCES

Abdallah, A. (2016): Precise Point Positioning for Kinematic Applications to Improve Hydrographic Survey, PhD, Stuttgart University, Stuttgart, Germany.

Abdallah, A., Schwieger, V. (2015): Kinematic Precise Point Positioning (PPP) Solution for Hydrographic Applications. FIG Congress 2015, 17-21 May, Sofia, Bulgaria.

Böder, V. (2010): Applications for a Hydrographic Multi-Sensor System on Lakes and Rivers. FIG Congress, 11-16 April, Sydney, Australia.

Dach, R., Hugentobler, U., Fridez, P., Meindl, M. (Eds) (2007): Bernese GPS Software Version 5.0. User manual. AIUB-Astronomical Institute, University of Bern, Switzerland.

Dach, R., Walser, P. (2015): Bernese GNSS Software Version 5.2 Tutorial. Available at: http://www.bernese.unibe.ch/docs/ TUTORIAL.pdf, last access on April, 2015.

El-Rabbany, A. (2002): Introduction to GPS, the Global Positioning System. Artech House communication series, Library of Congress, USA.

Erener, A., Gökalp, E. (2004): Mapping the Sea Bottom Using RTK GPS and Lead-Line in Trabzon Harbor. FIG Working Week, Athens, Greece.

Héroux, P., Kouba, J. (2001): GPS Precise Point Positioning Using IGS Orbit Products. Physics and Chemistry of the Earth, Part A: Solid Earth and Geodesy, 26(6-8).

Hoffmann-Wellenhof, B., Lichtenegger, H., Collins, J. (2000): GPS: Theory and Practice. 4th edition, Springer-Verlag/Wien New York.

Michaud, S., Morse, B., Santerre, R., Taschereau, A., Siles, J. (2002): Precise Determination of Vessel Squat and Under-Keel Clearance. 4th Transportation Specialty Conference of the Canadian Society for Civil Engineering, Montréal, Québec, Canada.

Mirsa, P., Enge, P. (2012): Global Positioning System Signals, Measurements, and Performance. Revised 2nd edition, Ganga-Jamuna Press, USA.

Niemeier, W. (2008): Ausgleichungsrechnung, Statistische Auswertemethoden. 2nd edition, Walter de Gruyter Berlin.New York.

Rizos, C. (2010): Making sense of the GNSS techniques. Chapter 11 In Manual of Geospatial Science and Technology, J. Bossler, J. Campbell, R. McMaster & C. Rizos, 2nd edition, Inc., Taylor & Francis.

SAPOS (2016): Satellitenpositionierungsdienst der Deutschen Landesvermessung. Available at: http://www.sapos.de/, last access on February, 2015.

SAPOS-NRW (2016): SAPOS- Nordrhein-Westfalen . Available at: http://www.bezreg-koeln.nrw.de/brk_internet/geobasis/raumbezug/sapos/index.html, last access on February, 2016

BIOGRAPHICAL NOTES

Dr. –Ing. **Ashraf Abdallah**

1998 – 2003 Studies of Civil Engineering in Aswan (University of Aswan, Egypt)
2005 – 2009 Research associate in Civil Engineering in Aswan (University of Aswan, Egypt)
2009 Master of Science (University of Aswan, Egypt)
2009 – 2011 Assistant lecturer in Civil Engineering in Aswan (University of Aswan, Egypt)
2012-2016 Ph. D. student at the Institute of Engineering Geodesy, University of Stuttgart
From 2016 Assistant Professor at the Faculty of Engineering, Aswan University, Egypt.

Prof. Dr.-Ing. habil. **Volker Schwieger**

1983 – 1989 Studies of Geodesy in Hannover
1989 Dipl.-Ing. Geodesy (University of Hannover)
1998 Dr.-Ing. Geodesy (University of Hannover)
2004 Habilitation (University of Stuttgart)
2010 Professor and Head of Institute of Engineering Geodesy, University of Stuttgart
2015 Chair of FIG Commission 5 ‘Positioning and Measurement’
2016 Dean of Faculty of Aerospace Engineering and Geodesy, University of Stuttgart

CONTACTS

Dr. –Ing. Ashraf Abdallah
Faculty of Engineering, Aswan University, Egypt.
81542 Aswan, Egypt
Email: ashraf.abdallah@aswu.edu.eg